

# Estimates of fluid pressure and tectonic stress in hydrothermal/volcanic areas: a methodological approach

Guido Ventura <sup>(1)</sup> and Giuseppe Vilardo <sup>(2)</sup>

<sup>(1)</sup> Istituto Nazionale di Geofisica e Vulcanologia, Roma, Italy

<sup>(2)</sup> Istituto Nazionale di Geofisica e Vulcanologia, Osservatorio Vesuviano, Napoli, Italy

## Abstract

An analytical approach to estimate the relative contribution of the fluid pressure and tectonic stress in hydrothermal/volcanic areas is proposed assuming a Coulomb criterion of failure. The analytical procedure requires the coefficient of internal friction, cohesion, rock density, and thickness of overburden to be known from geological data. In addition, the orientation of the principal stress axes and the stress ratio must be determined from the inversion of fault-slip or seismic data (focal mechanisms). At first, the stress magnitude is calculated assuming that faulting occurs in 'dry' conditions (fluid pressure=0). In a second step, the fluid pressure is introduced performing a grid search over the orientation of 1) fault planes that slip by shear failure or 2) cracks that open under different values of fluid pressure and calculating the consistency with the observed fault planes (*i.e.* strike and dip of faults, cracks, nodal planes from focal mechanisms). The analytical method is applied using fault-slip data from the Solfatara volcano (Campi Flegrei, Italy) and seismic data (focal mechanisms) from the Vesuvius volcano (Italy). In these areas, the fluid pressure required to activate faults (shear fractures) and cracks (open fractures) is calculated. At Solfatara, the ratio between the fluid pressure and the vertical stress  $\lambda$  is very low for faults ( $\lambda=0.16$ ) and relatively high for cracks ( $\lambda=0.5$ ). At Vesuvius,  $\lambda=0.6$ . Limits and uncertainties of the method are also discussed.

**Key words** *hydrothermal fluids – faults – cracks – fluid pressure – volcanic/hydrothermal areas – seismicity – Vesuvius – Campi Flegrei*

## 1. Introduction

Faults and fractures play a major role in the localization and evolution of hydrothermal flow (Sibson, 1996; Curewitz and Karson, 1997; Riedel *et al.*, 2001). This follows from the nearly ubiquitous close association of faults and hydrothermal outflows sites, which include hot

springs, geysers, fumaroles, and diffuse degassing areas (Chiodini *et al.*, 2001a; Craw *et al.*, 2002; Minissale, 2003; Molin *et al.*, 2003). Similar evidence for fault control on hydrothermal activity is the close association between faults and mineral deposits (*e.g.*, gypsum, anhydrite, quartz) arranged in veins or aligned spots (Hannington *et al.*, 2001; Singleton and Criss, 2002; Clark and James, 2003). Fluids may also play a major role in triggering seismicity (Sibson, 2000; Collettini, 2002; Tenthorey *et al.*, 2003). As faults propagate, interact and link, hydrothermal circulation may evolve from scattered migrating outflow sites to stable discharge sites affecting a fault or the whole fault system. Changes in the behavior of hydrothermal outflows near faults may reflect the evolution of the fault zone or of the hydrothermal systems (Chiodini *et al.*, 2001a; Molin, 2003). Then, the estimate of the fluid

*Mailing address:* Dr. Guido Ventura, Istituto Nazionale di Geofisica e Vulcanologia, Via di Vigna Murata 605, 00143 Roma, Italy; e-mail: ventura@ingv.it

pressure required to activate a fault or a crack and of the tectonic stress field acting on a fault is of primary importance for the study of 1) active hydrothermal systems or paleo-flow systems and b) the analysis of the hydraulic structure of fault zones. This also has implications for the study of the hazard related to the seismic, volcanic, and hydrothermal activity (Sibson, 1998; Saccorotti *et al.*, 2001; Finizola *et al.*, 2002).

In this study, we propose an analytical method to obtain semi-quantitative estimates of the magnitude of tectonic stress and fluid pressure in fault zones. The method is based on the collection and elaboration (stress inversion) of structural data and/or data from focal mechanisms and allow us to estimate the magnitude of the principal tectonic stress ( $\sigma_1$ ,  $\sigma_2$ , and  $\sigma_3$ ) and fluid pressure  $P_f$  in active hydrothermal/tectonic areas. Examples of application to areas characterized by extensional (Solfatara volcano, Campi Flegrei, Italy) and strike-slip tectonics (Vesuvius, Italy) are provided and the results are discussed.

## 2. Analytical method

Jaeger and Cook (1979) present an equation that shows the criteria for Coulomb shear failure along a plane. Rewriting their equation in terms of  $\theta$ , the angle that the greatest principal stress  $\sigma_1$  makes with the plane of weakness gives (Fournier, 1996)

$$(\sigma_1 - \sigma_3) = \frac{[2\mu\sigma_3 + 2C]}{[(1 - \mu \tan \theta) \sin 2\theta]} \quad (2.1)$$

where  $\mu$  is the coefficient of internal friction and  $C$  is the cohesion,

Note that eq. (2.1) is valid if the fluid pressure  $P_f=0$ . If  $P_f \neq 0$ ,  $\sigma_1$ ,  $\sigma_2$ ,  $\sigma_3$  may be determined assuming a Coulomb criterion of failure and resolving the system of equations

$$(\sigma_1 - \sigma_3) = \frac{[2\mu(\sigma_3 - \lambda\sigma_v) + 2C]}{[(1 - \mu \tan \theta) \sin 2\theta]} \quad (2.2)$$

$$\sigma_1 = \rho gh \text{ (normal stress regime), or} \quad (2.3a)$$

$$\sigma_2 = \rho gh \text{ (strike-slip regime), or} \quad (2.3b)$$

$$\sigma_3 = \rho gh \text{ (compressive regime)} \quad (2.3c)$$

$$R = \frac{(\sigma_2 - \sigma_3)}{(\sigma_1 - \sigma_3)} \quad (2.4)$$

$$\mu = \frac{1}{\tan 2\theta}; \quad \lambda = \frac{P_f}{\sigma_v} \quad (2.5)$$

where  $\rho$  is the rock density,  $g$  is the acceleration of gravity,  $h$  is the thickness of overburden. This system may be resolved if a)  $\rho$  and  $h$  are known from geological data; b)  $R$  and the orientation of the principal stress axes are known from inversion of fault-slip data or focal mechanisms of earthquakes; and c)  $\theta$  is determined from the angular relationships between the maximum principal stress and the preferred rupture plane(s). The analytical procedure to solve the system consists of three main steps. In a first step, the stress magnitude is calculated setting  $\lambda=0$  and  $C=0$ , and assuming that faulting occurs on pre-existing planes of weakness. In a second step,  $P_f$  is introduced performing a grid search over the orientation of fault planes that slip by shear failure under different values of  $\lambda$  and calculating the consistency with the observed fault planes (*e.g.*, strike and dip of nodal planes from focal mechanisms) following the procedure of Morris *et al.* (1996) and Phillips *et al.* (1997). In this step and in the next step,  $C$  and  $\mu$  are unchanged. In a third step,  $P_f$  is varied performing a grid search over the orientation of planes that shear under different values of  $\lambda$  and calculating the consistency with the measured (faults) or determined (focal mechanisms) rupture planes. Here below, this method is applied using structural data from the Solfatara crater (Campi Flegrei, Italy) and seismic data (focal mechanisms) from the Vesuvius volcano (Italy). In these areas, the fluid pressure required to activate faults (shear fractures) and cracks (open fractures) is calculated.

## 3. Application

### 3.1. Solfatara crater (Campi Flegrei)

The Campi Flegrei is a nested caldera resulting from two large collapses related to the Cam-

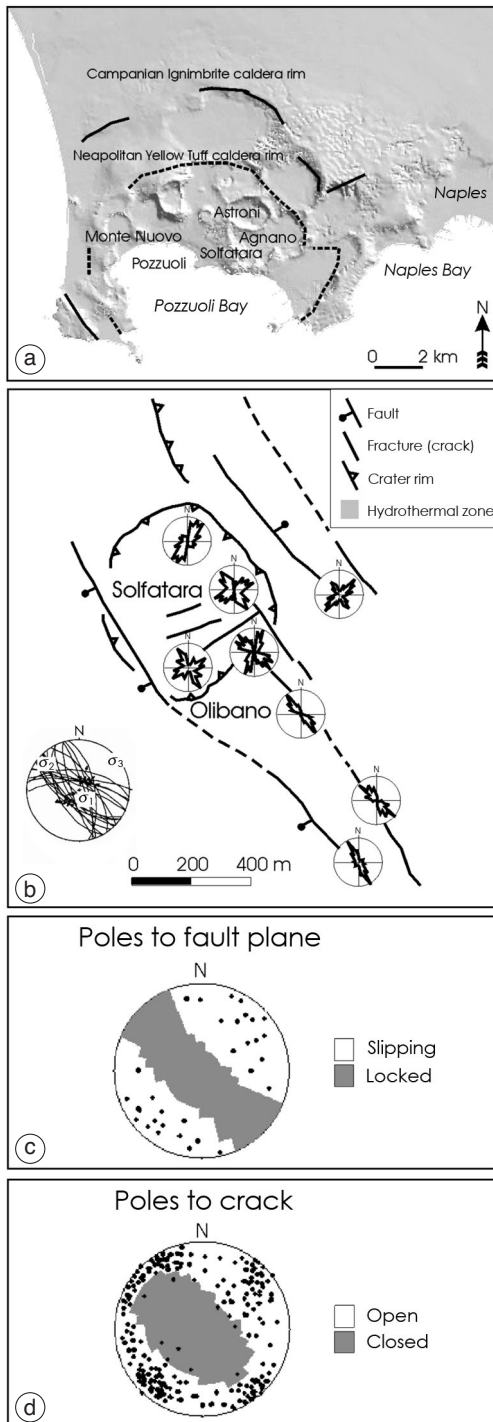


**Fig. 1a-d.** a) Sketch map of the Campi Flegrei caldera (from Orsi *et al.*, 1996). b) Structural map of the Solfatara area and summary of the mesostructural measurement in the Solfatara area. Fault-slip data and orientation of the stress axes are reported right down (Schmidt net, lower hemisphere projection; data from Chiodini *et al.*, 2001). The azimuthal distribution of the strike of cracks in different selected sites is plotted on Rose diagrams. Each measurement site does not exceed 40 m<sup>2</sup>. c, d) Results of the stress field analysis on the Solfatara faults (c;  $\lambda=0.16$ ) and cracks (d;  $\lambda=0.5$ ). Poles to measured fault planes (upper panel) and crack walls (lower panel) are reported as dots (Schmidt net, lower hemisphere).

panian Ignimbrite (39 kyr) and to the Neapolitan Yellow Tuff (12 kyr) eruptions (fig. 1a; Orsi *et al.*, 1996). The Campi Flegrei magmatic system is still active and the last eruption occurred in 1538 A.D. at Monte Nuovo. Faults affecting the Campi Flegrei caldera follow two preferred strikes, NW-SE and NE-SW, which are the same as the faults affecting the Campanian Plain and the inner sectors of the Apennine belt (Hippolyte *et al.*, 1994; Orsi *et al.*, 1996). The Solfatara volcano (180 m a.s.l.; fig. 1b) is a 3.8 to 4.1 kyr old tuff-cone located NE of Pozzuoli.

The Solfatara crater is affected by two main faults striking NW-SE. Outside the crater area, two NW-SE striking faults cut the eastern sector of the tuff cone (fig. 1b). The Solfatara NW-SE striking fault segments show a maximum measured vertical offset equal to 40 m on the SW corner of the crater. In the crater area, NE-SW and NW-SE striking cracks and fluid-filled veins occur (fig. 1b). Results of a mesostructural study carried out to characterize the Solfatara deformation pattern show that the faults have normal slips with pitch  $\geq 75^\circ$ . They move in response to a normal stress field characterized by a sub-vertical  $\sigma_1 = \sigma_V$  (strike  $264^\circ$ , plunge  $79^\circ$ ) and a NE-SW striking subhorizontal  $\sigma_3$  (strike  $45^\circ$ , plunge  $8^\circ$ ) (fig. 1b).  $\sigma_2$  (strike  $316^\circ$ , plunge  $7^\circ$ ) parallels the NW-SE fault strike and  $R=0.18$  (Chiodini *et al.*, 2001a). This stress configuration is consistent with that obtained by Zuppetta and Sava (1993) from the analysis of focal mechanisms of earthquakes which occurred in 1982-1984.

To verify if the fluid pressure plays a role in the kinematics of the Solfatara faults, the above

described procedure is applied. In a first step, we set  $\lambda=0$  and  $\rho=2000 \text{ kg/m}^3$  (average density of the Flegrei pyroclastics; Barberi *et al.*, 1991).  $\mu$  was determined measuring the angle  $\theta$  between the fault planes and the orientation of  $\sigma_1$  determined from the inversion of fault-slip data, *i.e.*  $\theta \sim 30^\circ$ .  $C$  was set to zero assuming that faulting occurs on pre-existing planes of weakness. This assumption is justified by the fact that the Solfatara faults follow the same trend as the main structural discontinuity affecting the Campi Flegrei caldera.

In a second step, we introduce  $P_f$  performing a grid search over the orientation of fault planes that slip by shear failure under different values of  $\lambda$  and calculated the consistency with the NW-SE fault planes following the method of Morris *et al.* (1996). Both  $C$  and  $\mu$  are unchanged. The obtained results (fig. 1c) indicate that 1) at  $P_f=0$ , the variation of the stress magnitude with depth is  $\Delta\sigma_1=20 \text{ MPa/km}$ ,  $\Delta\sigma_2=9 \text{ MPa/km}$  and  $\Delta\sigma_3=6.7 \text{ MPa/km}$ ; 2) the differential stress is about 13 MPa at 1 km of depth; and 3)  $P_f$  required to activate the NW-SE faults is 3.3 MPa/km (fig. 1c). As a result,  $\lambda=0.16$ . The effective stress magnitude ( $\sigma_{1\text{eff}}=\sigma_1-P_f$ ;  $\sigma_{2\text{eff}}=\sigma_2-P_f$ ;  $\sigma_{3\text{eff}}=\sigma_3-P_f$ ) are:  $\sigma_{1\text{eff}}=17 \text{ MPa/km}$ ,  $\sigma_{2\text{eff}}=6 \text{ MPa/km}$  and  $\sigma_{3\text{eff}}=3.7 \text{ MPa/km}$ . We conclude that fluids play a minor role in the kinematics of the Solfatara faults. However, both NE-SW and NW-SE cracks and fluid-filled veins occur within the crater area. Then, we vary  $P_f$  performing a grid search over the orientation of planes that open (cracks) under different values of  $\lambda$  and calculating the consistency with the measured crack parameters (strike and dip of crack wall). Results indicate that  $P_f$  required to open both the NW-SE and NE-SW cracks is of about 10 MPa/km (fig. 1d). The calculated  $\lambda$  value is 0.5. In summary, the obtained results indicate that  $P_f < \sigma_3$  is required to activate the NE-SW faults by shear, whereas  $\sigma_2 - P_f > \sigma_3$  is required to open the NE-SW and NW-SE striking cracks.

### 3.2. Vesuvius volcano

Vesuvius volcano has been in a quiescent stage since 1944 and is characterized by a low temperature fumarolic activity ( $T_{\text{max}}=100^\circ\text{C}$ ).

The Vesuvius cone is located within a caldera formed during both sub-plinian (*e.g.* 1631; Rosi *et al.*, 1993) and plinian eruptions (*e.g.* 79 A.D.; Santacroce, 1987). Two main fault systems striking NW-SE and NE-SW affect the volcanic edifice. Vesuvius seismicity (about 200 events/yr;  $-0.4 \leq M_D \leq 3.6$ ) concentrates within the caldera volume and is characterized by swarm type sequences. The hypocentral depths range from the top of the volcanic edifice up to about 6 km b.s.l. (fig. 2a). Maximum event clustering occurs between 2 and 3 km b.s.l., at the interface between the sedimentary basement of the volcano (limestones and dolomites) and the intra-caldera volcanic rocks (fig. 2a; Cassano and La Torre, 1987), and where the present-day hydrothermal system is located (Chiodini *et al.*, 2001b). Available focal mechanisms show prevailing strike-slip solutions (Vilardo *et al.*, 1996). Correlations between the annual pattern exhibited by the time series of the events number and the seismic energy release indicate that pore pressure variations due to diffusion processes within the hydrothermal system are responsible for the lubrication of pre-existing fractures, so triggering seismicity (Vilardo *et al.*, 1999; Saccorotti *et al.*, 2002).

The stress field acting within the Vesuvius volcano was determined by Bianco *et al.* (1998) and Vilardo *et al.* (1999) using focal mechanisms from 1996-1997 time period. The inversion of 60 focal mechanisms of events located at depth between +1 and -6 km a.s.l. and  $M_D$  between 1 and 3.2 show that the Vesuvius stress field is heterogeneous. However, the majority of the solutions are consistent with a prevailing strike-slip stress field characterized by subhorizontal WNW-ESE  $\sigma_1$ , NNE-SSW  $\sigma_3$  and subvertical  $\sigma_2$ . According to Bianco *et al.* (1998), this configuration reflects the action of the regional stress field on the volcano. Here, the 35 available focal mechanisms of events with  $M_D \geq 1.5$  which occurred between 2 and 5 km b.s.l. from the data set of Vilardo *et al.* (1999), which refers to 1996-1997 seismicity, are selected. The fault plane solutions are characterized by subvertical nodal planes following two main strikes: NNW-SSE and NE-SW (fig. 2b). The inversion (Sperner *et al.*, 1993) of the selected

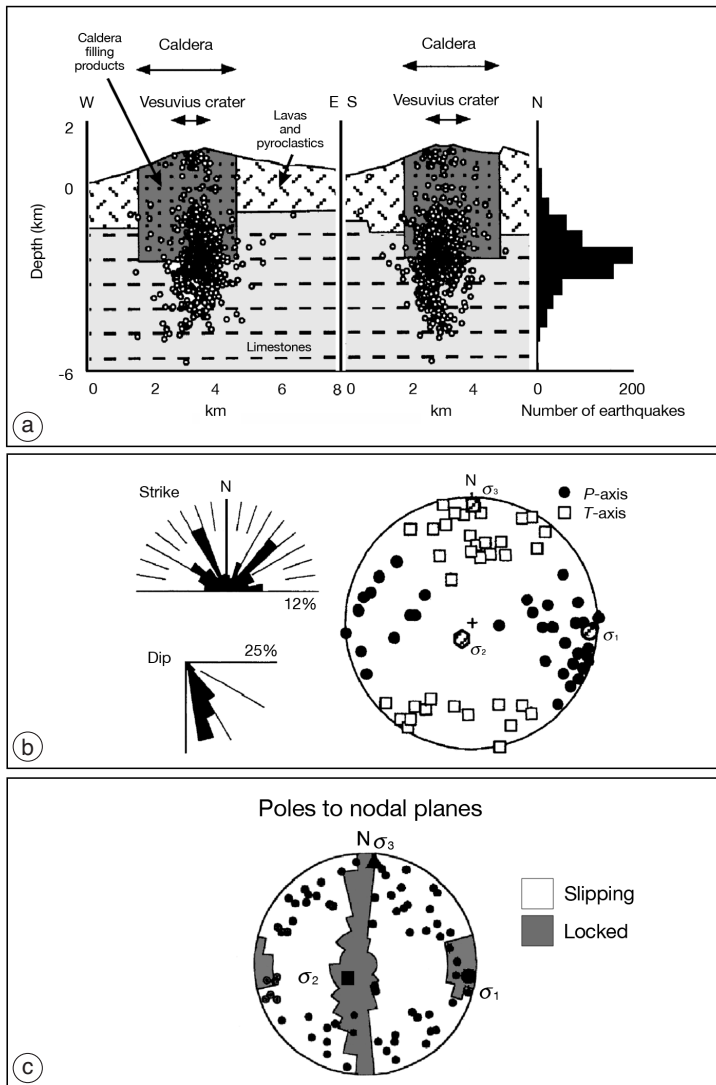


**Fig. 2a-c.** a) Schematic cross sections of the Vesuvius volcano (from Cassano and La Torre, 1987, modified) with circles representing the hypocentral location of the 1986-1997 earthquakes. Number of events *versus* depth is also reported. b) Azimuthal distribution of angular parameters of nodal planes from 35 focal mechanisms of earthquakes with  $M_D \geq 1.5$  occurred in 1996-1997 period, and distribution of *P* and *T* axes and of the principal stress axes. c) Results of the stress field analysis on the nodal planes from earthquakes ( $\lambda=0.6$ ).

fault plane solutions is consistent with a strike-slip stress configuration characterized by  $\sigma_1=91^\circ$  and  $7^\circ$  (trend and plunge),  $\sigma_2=219^\circ$  and  $79^\circ$ ,  $\sigma_3=360^\circ$  and  $8^\circ$  (fig. 2b), and  $R=(\sigma_2+$

$-\sigma_3)/(\sigma_1-\sigma_3)=0.24$ . In a first step, we calculate stress magnitude in depth by setting  $\sigma_V=\sigma_2$  (strike-slip configuration),  $\lambda=0$  and  $\rho=2600$   $\text{kg/m}^3$  (mean density of the Vesuvius lavas;

Cassano and La Torre, 1987).  $\mu$  was determined measuring the angle  $\theta$  between the strike of nodal planes and the orientation of  $\sigma_1$ .  $C$  was set to zero assuming that faulting occurs on pre-existing planes of weakness. This assumption is justified by the fact that the nodal planes follow the same trends as the main structural discontinuity affecting the volcano basement. In a second step, we introduced  $P_f$  performing a grid search over the orientation and slip direction of planes which slipped under different values of  $\lambda$  and calculating the consistency with the nodal planes following the procedure of Morris *et al.* (1996) and Phillips *et al.* (1997). The results obtained (fig. 2c) are:  $\mu=0.18$  and  $\lambda=0.6$ . Effective principal stresses ( $\sigma_{1\text{eff}}=\sigma_1-P_f$ ;  $\sigma_{2\text{eff}}=\sigma_2-P_f$ ;  $\sigma_{3\text{eff}}=\sigma_3-P_f$ ) vary with depth with the following gradients:  $\Delta\sigma_{1\text{eff}}=17.3$  MPa/km,  $\Delta\sigma_{2\text{eff}}=10$  MPa/km and  $\Delta\sigma_{3\text{eff}}=7.6$  MPa/km. We conclude that fluid pressure plays a major role in triggering Vesuvius seismicity.

#### 4. Discussion and conclusions

The proposed analytical method is based on the assumption that some geotechnical data (*e.g.*, cohesion; density) of the rocks are known. In the above reported examples, we assume that faulting occurs on pre-existing zones of discontinuity and set  $C=0$ . However, this may be not true in hydrothermal zones, where self-sealing processes in fractures are common and mineral-filled fractures (veins) may act as barriers to fluid flow (*e.g.*, Thentorey *et al.*, 2003). In addition, we assume no variations of density with depth. In the cases of Vesuvius and Campi Flegrei, this is a reasonable assumption because significant variations in density with depth are lacking at least in the first 2-3 km below the volcano axis (Cassano and La Torre, 1987; Rosi and Sbrana, 1987). However, this may be an over-simplification in many hydrothermal and/or volcanic areas because of the occurrence of strong layering within both the shallow and deeper parts of the crust. An additional problem concerns the occurrence of areas subjected to heterogeneous stress sources. This is the case of volcanoes, whose structural features generally result from the superimposition of gravity, tec-

tonic and magmatic induced stress. In this picture, a procedure of data selection must be implemented to select brittle structures related to tectonic and fluid-induced stresses alone, without the contribution of gravity. Taking into account the above reported limitations, the results of analysis presented here may give useful information on the relative contribution of tectonic stress and fluid pressure in triggering faulting and cracking in volcanic/hydrothermal areas. Examples from Solfatara and Vesuvius show that hydrothermal fluids play a major role in triggering Vesuvius seismicity and in opening of the Solfatara cracks, whereas they play a minor role in the dynamics of the Solfatara faults. In particular, the Solfatara cracks may open only by fluid overpressure, *i.e.* by hydrofracturing. These results are consistent with the conclusions from independent geochemical and seismological studies on Solfatara and Vesuvius (Chiodini *et al.*, 2001a,b; Saccorotti *et al.*, 2001, 2002). The analytical method proposed here may be applied to other non-volcanic areas where there is geophysical/geological evidence of fluid involvement (Colletini, 2002).

#### Acknowledgements

We are grateful to Giovanni Chiodini, Gilberto Saccorotti and Edoardo Del Pezzo for the numerous discussions about the problems of hydraulic fracturing and tectonic stress in hydrothermal/volcanic areas. We also thank Laura Crispini for review of an early version of the manuscript and Roberto Moretti for the editorial handling.

#### REFERENCES

- BARBERI, F., E. CASSANO, P. LA TORRE and A. SBRANA (1991): Structural evolution of Campi Flegrei caldera in light of volcanological and geophysical data, *J. Volcanol. Geotherm. Res.*, **48**, 33-49.
- BIANCO, F., M. CASTELLANO, G. MILANO, G. VENTURA and G. VILARDO (1998): The Somma-Vesuvius stress field induced by regional tectonics: evidences from seismological and mesostructural data, *J. Volcanol. Geotherm. Res.*, **82**, 199-218.
- CASSANO, E. and P. LA TORRE (1987): Geophysics, in *Somma-Vesuvius*, edited by R. SANTACROCE, *Quad. Ric. Sci.*, **114**, 175-195.

- CHIODINI, G., F. FRONDI, C. CARDELLINI, D. GRANIERI, L. MARINI and G. VENTURA (2001a): CO<sub>2</sub> degassing and energy release at Solfatara volcano, Campi Flegrei, Italy, *J. Geophys. Res.*, **106** (B8), 16,213-16,222.
- CHIODINI, G., L. MARINI and M. RUSSO (2001b): Geochemical evidence for the existence of high-temperature hydrothermal brines at Vesuvio volcano, Italy, *Geochim. Cosmochim. Acta*, **65**, 2129-2147.
- CLARK, C. and P. JAMES (2003): Hydrothermal brecciation due to fluid pressure fluctuations: examples from the Olary Domain, South Australia, *Tectonophysics*, **366**, 187-206.
- COLLETTINI, C. (2002): Hypothesis for the mechanics and seismic behaviour of low-angle normal faults: the example of the Altotiberina Fault Northern Apennines, *Ann. Geophysics*, **45** (5), 683-698.
- CRAW, D., P.O. KOONS, T. HORTON and C.P. CHAMBERLAIN (2002): Tectonically driven fluid flow and gold mineralisation in active collisional orogenic belts: comparison between New Zealand and Western Himalaya, *Tectonophysics*, **348**, 135-153.
- CUREWITZ, D. and J.A. KARSON (1997): Structural settings of hydrothermal outflow: fracture permeability maintained by fault propagation and interaction, *J. Volcanol. Geotherm. Res.*, **79**, 149-168.
- FINIZOLA, A., F. SORTINO, J.F. LÉNAT and M. VALENZA (2002): Fluid circulation at Stromboli volcano (Aeolian Islands, Italy) from self-potential and CO<sub>2</sub> surveys, *J. Volcanol. Geotherm. Res.*, **116**, 1-18.
- FOURNIER, R. (1996): Compressive and tensile failure at high fluid pressure where preexisting fractures have cohesive strength, with application to the San Andreas Fault, *J. Geophys. Res.*, **101** (B11), 25499-25509.
- HANNINGTON, M., P. HERZIG, P. STOFFERS, J. SCHOLTEN, R. BOTZ, D. GARBE-SCHÖNBERG and I.R. JONASSON (2001): First observations of high-temperature submarine hydrothermal vents and massive anhydrite deposits off the north coast of Iceland, *Mar. Geol.*, **177**, 199-220.
- HIPPOLYTE, J.C., J. ANGELIER and F. ROURE (1994): A major geodynamic change revealed by Quaternary stress patterns in the Southern Apennines (Italy), *Tectonophysics*, **230**, 199-210.
- JAeger, J. and N.G.W. COOK (1979): *Fundamental of Rock Mechanics* (Chapman & Hall, London), 3rd edition, pp. 593.
- MINISSALE, A., D. CHANDRASEKHARAM, O. VASELLI, G. MAGRO, F. TASSI, G.L. PANSINI and A. BHRAHABUT (2003): Geochemistry, geothermics and relationship to active tectonics of Gujarat and Rajasthan thermal discharges, India, *J. Volcanol. Geotherm. Res.*, **127** (1-2), 19-32.
- MOLIN, P., V. ACOCELLA and R. FUNICIELLO (2003): Structural, seismic and hydrothermal features at the border of an active intermittent resurgent block: Ischia Island (Italy), *J. Volcanol. Geotherm. Res.*, **121**, 65-81.
- MORRIS, A., D.A. FERRILL and D.B. HERDERSON (1996): Slip-tendency analysis and fault reactivation, *Geology*, **24**, 275-278.
- ORSI, G., S. DE VITA and M. DI VITO (1996): The restless, resurgent Campi Flegrei nested caldera (Italy): constraints on its evolution and configuration, *J. Volcanol. Geotherm. Res.*, **74**, 179-214.
- PHILLIPS, W.S., L.S. HOUSE and M.C. FEHLER (1997): De-tailed joint structure in a geothermal reservoir from studies of induced microearthquake clusters, *J. Geophys. Res.*, **102**, 11745-11763.
- RIEDEL, C., M. SCHMIDT, R. BOTZ and F. THEILEN (2001): The Grimsey hydrothermal field offshore North Iceland: crustal structure, faulting and related gas venting, *Earth Planet. Sci. Lett.*, **193**, 409-421.
- ROSI, M. and A. SBRANA (1987): Phlegraean Fields, *Quad. Ric. Sci.*, **9**, pp. 175.
- ROSI, M., C. PRINCIPE and R. VECCI (1993): The 1631 Vesuvius eruption. A reconstruction based on historical and stratigraphical data, *J. Volcanol. Geotherm. Res.*, **58**, 155-182.
- SACCOROTTI, G., F. BIANCO, M. CASTELLANO and E. DEL PEZZO (2001): The July-August 2000 seismic swarms at Campi Flegrei volcanic complex, Italy, *Geophys. Res. Lett.*, **28**, 2525-2528.
- SACCOROTTI, G., G. VENTURA and G. VILARDO (2002): Seismic swarms related to diffusive processes: the case of Somma-Vesuvius volcano, Italy, *Geophysics*, **67** (1), 199-203.
- SANTACROCE, R. (Editor) (1987): Somma-Vesuvius, *Quad. Ric. Sci.*, **114** (8), 1-251.
- SIBSON, R.H. (1996): Structural permeability of fluid-driven fault-fracture meshes, *J. Struct. Geol.*, **18**, 1031-1042.
- SIBSON, R.H. (1998): Brittle failure mode plots for compressional and extensional tectonic regimes, *J. Struct. Geol.*, **20**, 655-660.
- SIBSON, R.H. (2000): Tectonic controls on maximum sustainable overpressure: fluid redistribution from stress transitions, *J. Geochem. Explor.*, **69**, 471-475.
- SINGLETON, M.J. and R.E. CRISS (2002): Effects of normal faulting on fluid flow in an ore-producing hydrothermal system, Comstock Lode, Nevada, *J. Volcanol. Geotherm. Res.*, **115**, 437-450.
- SPERNER, B., L. RATSCHBACHER and R. OTT (1993): Fault-striae analysis: a Turbo Pascal program package for graphical presentation and reduced stress tensor calculation, *Comput. Geosci.*, **19**, 1361-1388.
- TENTHOREY, E., S. COX and F.F. TODD (2003): Evolution of strength recovery and permeability during fluid-rock reaction in experimental fault zones, *Earth Planet. Sci. Lett.*, **206**, 161-172.
- VILARDO, G., G. DE NATALE, G. MILANO and U. COPPA (1996): The seismicity of Mt. Vesuvius, *Tectonophysics*, **261**, 127-138.
- VILARDO, G., G. VENTURA and G. MILANO (1999): Factors controlling the seismicity of the Somma Vesuvius volcanic complex, *Volcanol. Seismol.*, **20**, 219-238.
- ZUPPETTA, A. and A. SAVA (1993): Stress pattern at Campi Flegrei from focal mechanisms of the 1982-1984 earthquakes (Southern Italy), *J. Volcanol. Geotherm. Res.*, **48**, 127-137.